The Luminosity Profile and Structural Parameters of M31

S. Courteau[1], L.M. Widrow[1], M. McDonald[2], P. Guhathakurta[3], K. Gilbert[4], etal.*

[1]Queen's University, Kingston, ON, Canada; [2]Kavli Institute/MIT, Cambridge, MA, USA; [3]UCSC/Lick, Santa Cruz, CA; [4]UWash, Seattle, Wash.

Summary: We present a composite luminosity profile for the Andromeda galaxy, M31, which covers four decades in projected radius. The profile is decomposed into three components: a bulge, a disk, and a stellar halo. Our paper addresses different decomposition methods to 1D luminosity profiles and 2D images as well as their limitations. The stellar nucleus, bulge, disk, and halo components each contribute ~0.05%, 23%, 73%, and 4% of the total light of M31 out to 200 kpc along the minor axis.

Composite Minor-Axis Profile

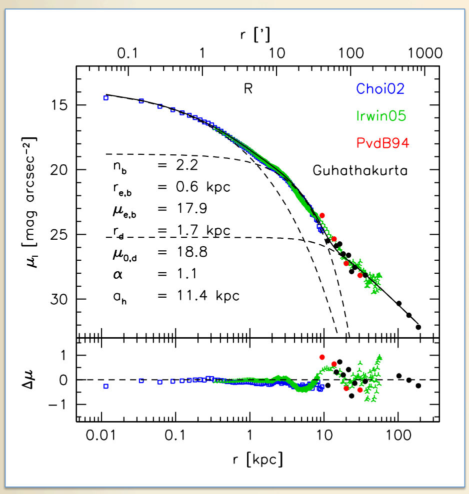

Fig. 1. − Composite minor-axis profile of M31. The I-band minor-axis brightnesses, shown in blue, were extracted from the I-band image of Choi et al. (2002). Extension of the Choi02 profile relies on the star counts of M31's stellar halo largely along the minor axis by Irwin et al. (2005), Pritchet & van den Bergh (1994), and Gilbert et al. (2009). The Irwin05 error bars were re-derived by us.

We provide an investigation of luminosity profile decomposition methods. The inferred structural parameters depend on whether the data are spatially binned or not, treated in magnitudes or counts, and clipped for non-axisymmetric features, and whether we analyse wedges (cuts), an azimuthally-averaged profile, or a 2D image. The combination with kinematic data may also yield different results (Dorman etal 2012). **Fig. 1 shows our "best" decomposition of the M31 light in terms of a model bulge, disk and stellar halo.**

B/D Decomposition Results

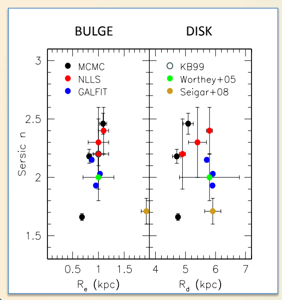

Fig. 2. − Distribution of model parameters for the Bulge/Disk decompositions of IRAC data (Barmby etal 2006). MCMC and NLLS models use 1D decompositions; GALFIT (Peng etal 2002) models use 2D decomps of IRAC images. **With n=2.2±0.3, the M31 bulge does not resemble a de Vaucouleurs spheroid.**

The left window shows our solutions plus those of Kormendy & Bender 1999, Worthey et al. (2005), and Seigar et al. (2008). The X-axes correspond to the face-on projection.

Light Fractions

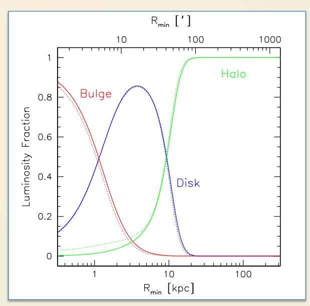

Fig. 3. − Projected light fraction of the bulge, disk, and halo components based on the composite luminosity profile (Fig. 1), as a function of projected radius. The solid and dotted lines represent two MCMC models (see paper). The bulge and disk light fractions are equal just beyond 1 kpc along the minor axis; the disk and halo light fractions reach equality between 7 and 9 kpc, depending on the model. **The stellar halo is dominant beyond 9 kpc.**

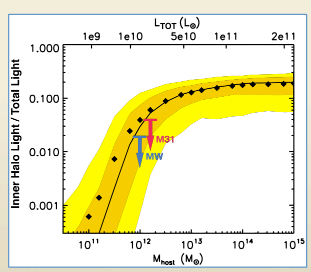

Fig. 4. − Prediction of the light fraction of the diffuse halo stars against the total galaxy light for a variety of accretion histories which account for much of the inner halo light, as a function of host halo mass (adapted from Purcell etal 2008). The blue and red arrows are the measured light fractions, ~2% and ~4%, for the Milky Way and M31, resp. Our results agree with a common evolution of the old stellar systems in the Milky Way and M31: **the inner regions (*R* ≤ *25 kpc*) would contain both accreted and in situ stellar populations while the outer regions (*R* ≥ *25 kpc*) would be assembled through pure accretion and the disruption of satellites** (see also Carollo et al. 2007, 2010; Purcell et al. 2008 and references therein).

* Courteau, S., Widrow, L.M., McDonald, M., Guhathakurta, P., Gilbert, K., Zhu, Y., Beaton, R.L., Majewski, S.R. 2011, ApJ, 739,20